

Article

Study on Sintering System of Calcium Barium Sulphoaluminate by XRD Quantitative Analysis

Jun Chang *, Xiaopeng Shang and Jiuye Zhao

School of Civil Engineering, Dalian University of Technology, Dalian 116024, China;

E-Mails: k@bw.com (X.S.); zhaojiuye89@126.com (J.Z.)

* Author to whom correspondence should be addressed; E-Mail: mlchang@dlut.edu.cn;
Tel./Fax: +86-0411-8470-7171.

Academic Editor: Wen-Hsiang Hsieh

Received: 18 August 2015 / Accepted: 20 October 2015 / Published: 2 November 2015

Abstract: Calcium barium sulphoaluminate (CBSA), derived from calcium sulphoaluminate (CSA), has excellent cementitious properties. In this study, the sintering system of CBSA with a theoretical stoichiometric $\text{Ca}_3\text{BaAl}_6\text{SO}_{16}$ was investigated. Rietveld refinement was performed using TOPAS 4.2 software to quantitatively calculate the content of CBSA and the actual ionic site occupancy of Ba^{2+} . The results indicate that the content of $\text{Ca}_{4-x}\text{Ba}_x\text{Al}_6\text{SO}_{16}$ increases with increasing sintering temperature in the 1200–1400 °C ranges. When sintered at 1400 °C for 180 min, the content of CBSA reaches 88.4%. However, CBSA begins to decompose at 1440 °C, after which the content decreases. The replacement rate of Ba^{2+} was also enlarged by increasing sintering temperature and prolonged sintering time. Sintering at 1400 °C for 180 min is considered as the optimum when replacement rate of Ba^{2+} and the content of CBSA were taken into account. $\text{Ca}_{3.2}\text{Ba}_{0.8}\text{Al}_6\text{SO}_{16}$ with a content of 88.4% was synthesized.

Keywords: calcium barium sulphoaluminate; sintering system; Ba^{2+} replacement rate; Rietveld refinement

1. Introduction

Calcium barium sulphoaluminate (CBSA), derived from calcium sulphoaluminate (CSA), is the dominant mineral of sulphoaluminate cement and plays a decisive role in the performance of sulphoaluminate cement. The mineral properties of CBSA will be improved, and thereby the

performance of cement will also improve, when Ca ions are replaced by the Ba ions [1–4]. With the improvement of testing techniques and analysis software, Rietveld refinement can be used to study the atomic site occupancy, changes of lattice parameters, crystal structures and crystal phases during the solid solution reaction [5]. The results showed that the calcium sulphoaluminate could be cubic [6,7], tetragonal [8] and orthorhombic [9,10]. Hargis *et al.* refined the three crystal systems separately by Rietveld refinement and showed that the fitting result of the orthorhombic is the best [11]. Cuesta *et al.* indicated that CSA mineral could be orthorhombic and that orthorhombic crystal sometimes would transform into the cubic at around 470 °C [12,13]. Andac *et al.* also showed that crystal system transition occurred at around 470 °C [14]. Pinazo quantitatively analyzed the sulphoaluminate cement with orthorhombic and cubic CSA using Rietveld refinement methods [15].

With Rietveld refinement and highly qualified XRD data, quantitative phase analysis of the sintered products and atomic occupancy of barium ions can be obtained. In this paper, 1 mol barium ions was prepared to replace the calcium ions in CSA mineral and the minerals were sintered at 1200 °C, 1300 °C, 1350 °C, 1400 °C and 1440 °C, respectively, for 90 min, 120 min, 150 min and 180 min. Phase identification was carried out using Diffract EVA software (Bruker AXS, Berlin, Germany). Rietveld refinement was performed using TOPAS 4.2 software (Bruker AXS, Berlin, Germany) to quantitatively calculate the content of CBSA and the ionic occupancy of Ba²⁺. The optimum sintering system of CBSA and the effects of which on ionic occupancy of Ba²⁺ were investigated.

2. Experimental Section

2.1. Sample Preparation

Analytic chemical reagents calcium carbonate (CaCO₃), anhydrite calcium sulfate (CaSO₄), barium carbonate (BaCO₃) and neutral alumina (Al₂O₃) were used as raw materials. Quantities of 2 mol CaCO₃, 1 mol BaCO₃, 3 mol Al₂O₃ and 1 mol anhydrous CaSO₄ were mixed and ground for 10 min. Then the raw materials were pressed into round cakes (Φ 5 cm \times 1 cm) and were put into a high temperature furnace for sintering. The target temperatures were 1200 °C, 1300 °C, 1350 °C, 1400 °C and 1440 °C, respectively. The prolonged sintering time for each temperature was 90 min, 120 min, 150 min and 180 min. The minerals were cooled rapidly using a fan to the room temperature and then were ground for analysis after being sintered.

2.2. Test Methods

2.2.1. XRD Measurement

XRD Measurements were carried out by a Bruker AXSD8 Advance (Bruker AXS, Berlin, Germany) with Davinci X-ray ($\lambda = 1.5406 \text{ \AA}$, 40 kV and 40 mA, scan interval 10°–60° 2 θ , 0.01° and 1 s per step). The detector was lynxeye linear detector with an opening of 2.94°. The step size was 0.02° and the measurement time per step was 1 s. EVA software was used for phase determination.

2.2.2. Quantitative Phase Analysis and Atomic Site Occupancy Analysis

Rietveld refinement was employed by TOPAS 4.2 software for quantitative analysis and atomic site occupancy analysis. The Rietveld refinement strategy consisted of emission profile, background, instrument factors and zero error.

In the Rietveld refinement process, R_{wp} (radiation work permit) was used to evaluate the fitting results as shown in Equation (1). Generally, when R_{wp} is less than 15%, the result could be considered as reliable [16].

$$R_{wp} = \sum \{W_i [(y_i(\text{obs}) - y_i(\text{cal}))^2] / \sum w_i [y_i(\text{obs})^2]\}^{1/2} \quad (1)$$

where, R_{wp} indicates radiation work permit; $y_i(\text{obs})$ is the measured diffraction strength at the point $2\theta_i$ in the diffraction pattern; $y_i(\text{cal})$ presents the calculated diffraction strength at the point $2\theta_i$ in the diffraction pattern and w_i is weighting factor.

Lattice parameters, atomic coordinates, atomic site occupancy and temperature factors were considered in the refinement process.

Replacement rate (P) of Ba ions was introduced as Equation (2).

$$P = \left[\frac{\text{Ba}_c}{\text{Ba}_c + \text{Ca}_c} \right] \times W_c + \left[\frac{\text{Ba}_o}{\text{Ba}_o + \text{Ca}_o} \right] \times W_o \quad (2)$$

where, P presents the replacement rate of Ba ions; Ba_c and Ca_c are the occupancy rate of Ba ions and Ca ions in cubic yeelimite; Ba_o and Ca_o are the occupancy rate of Ba ions and Ca ions in orthorhombic yeelimite; W_c and W_o are the percentages of cubic yeelimite and orthorhombic yeelimite, respectively.

The replacement rate R (%) is defined as Equation (3).

$$R = (P \times 4) \times 100\% \quad (3)$$

where, R presents the replacement rate of Ba ion; P is the ionic site occupancy of Ba ion; 4 and 1 present the total cation and the number of Ba ion in theoretical $\text{Ca}_3\text{BaAl}_6\text{SO}_{16}$.

3. Results and Discussion

3.1. Qualitative Analysis of Minerals

The minerals sintered at 1200 °C, 1300 °C, 1350 °C, 1400 °C and 1440 °C for different times were analyzed by EVA software. The XRD patterns sintered for 180 min are shown in Figure 1 and the corresponding COD codes are listed in Table 1.

The diffraction peaks of CaO , BaSO_4 , $\text{Ca}_3\text{Al}_2\text{O}_6$, CaAl_2O_4 , $\text{Ca}_{12}\text{Al}_{14}\text{O}_{33}$, BaAl_2O_4 , CaSO_4 are obvious. When the sintering temperature is higher than 1100 °C, mesophases such as C12A7, CA, C4A3 could be formed in the sintering process [17,18]. The samples sintered at 1200 °C (Figure 2) show relatively messy peaks. The characteristic diffraction peaks of CBSA sintered at 1300 °C are relatively obvious and the characteristic peaks of mesophases decreased. The characteristic peaks of CBSA sintered at 1350 °C and 1400 °C are further strengthened and the mesophases reduced. The characteristic peaks of CBSA sintered at 1440 °C are obvious; however, the characteristic peaks of mesophases begin to increase due to the decomposition of CBSA.

Table 1. Phase and COD code.

Phase	COD code	Phase	COD code
CAS-Cubic	9009938	CA ₂	3500014
CAS-Orthorhombic	4001772	C ₄ A ₃	9002486
BA	1010630	C ₁₂ A ₇	4308078
BŠ	1010542	CŠ	9004096
CA	1528679	C	1011094

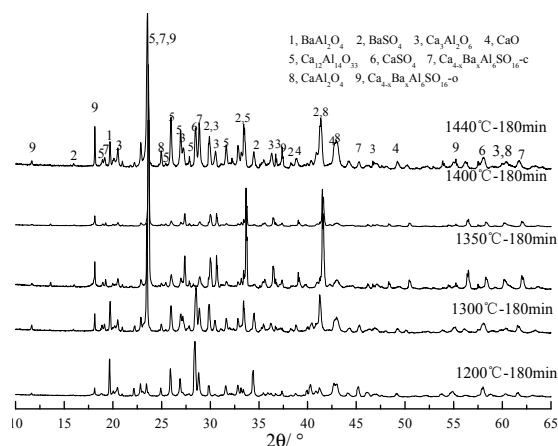


Figure 1. XRD Patterns of calcium barium sulphoaluminate (CBSA) samples sintered at different temperature for 180 min.

3.2. Quantitative Phase Analysis

According to the results of qualitative analysis, the structure documents of CaO, BaSO₄, Ca₃Al₂O₆, CaAl₂O₄, Ca₁₂Al₁₄O₃₃, BaAl₂O₄, CaSO₄ and Ca_{4-x}Ba_xAl₆SO₁₆ were imported into TOPAS 4.2 software for quantitative analysis. All the phases and corresponding ICSD codes are listed in Table 2. Ca_{4-x}Ba_xAl₆SO₁₆ is derived from Ca₄Al₆SO₁₆ and there is only a little offset at the diffraction peaks compared with that of Ca₄Al₆SO₁₆. The ICSD code of Ca₄Al₆SO₁₆ was used to refine the structure of Ca_{4-x}Ba_xAl₆SO₁₆. In the replacement process, the probability that Ca²⁺ at each position is replaced by Ba²⁺ is the same. The R_{wp} values are all less than 15, which indicate the quantitative analysis results are reliable.

Table 2. Phases and ICSD codes.

Phase	ICSD code	Phase	ICSD code
Ca ₄ Al ₆ SO ₁₆ -Cubic	9560	CaAl ₄ O ₇	16191
Ca ₄ Al ₆ SO ₁₆ -Orthorhombic	80361	Ca ₁₂ Al ₁₄ O ₃₃	261586
BaAl ₂ O ₄	246028	CaSO ₄	183919
BaO	186427	CaO	261847
CaAl ₂ O ₄	180997	-	-

The fitting effect of the sample sintered at 1400 °C for 180 min 1400 °C is presented in Figure 2. The result of raw data and fitting data has less error of fitting, it alligns nicely with the value of R_{wp}, which is 8.06. Unit cell parameters of CBSA samples sintered at 1200 °C, 1300 °C, 1350 °C, 1400 °C for 180 min

are presented in Table 3. As Table 3 shows, result of unit cell parameters indicated that the lattice constant increased with increasing sintering temperature. This phenomena can be attributed to the incorporation of Ba ions into the CSA crystal lattice because the atomic radius of barium is bigger than that of calcium. The same phenomena occurs when the soaking time of the same sintering temperature is increased.

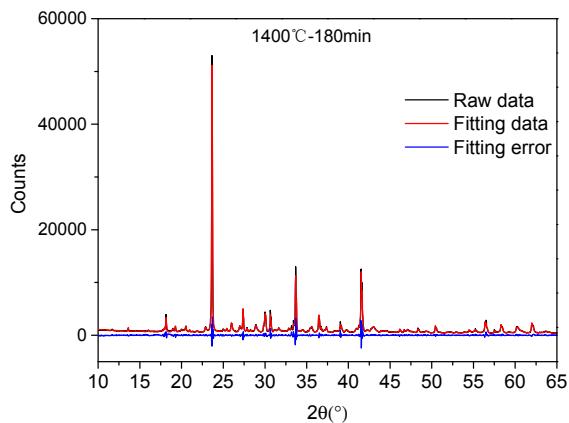


Figure 2. Fitting effect of CBSA samples sintered at 1400 °C for 180 min.

Table 3. Unit cell parameters of CBSA samples.

Phase	Parameter	1200 °C-180 min	1300 °C-180 min	1350 °C-180 min	1400 °C-180 min
CBSA-O	a	13.01032	13.0207508	13.0270247	13.0402404
	b	12.92488	12.9469589	12.9600426	12.9981782
	c	9.21658	9.22244	9.22428	9.2330302
CBSA-C	a	9.21896	9.22475	9.23109	9.23704

To illustrate the unit cell variation of different Ba incorporation, one pure CSA with full Ca content and a second one with half mole of Ba concentration were prepared. As Table 4 shows, *d* values of the main peak and the second peak were obtained. Phase analysis shows that the distance of crystal face of CBSA increase with the increasing of Ba ion implantation.

Table 4. *d* value of main peak and second peak.

Ba Content	Main Peak	Second Peak
	<i>d</i> value	<i>d</i> value
0	3.74749	2.65358
0.5	3.75387	2.97368
1.0	3.78612	3.12588

The total amount of orthorhombic and cubic CBSA is marked as $Ca_{4-x}Ba_xAl_6SO_{16}$ and the quantitative analysis results are presented in Figure 3. The total amount of $Ca_{4-x}Ba_xAl_6SO_{16}$ is 40%–50% when the sintering temperature between 1200 °C and 1300 °C. With the increase of prolonged time, the amount of $Ca_{4-x}Ba_xAl_6SO_{16}$ shows a negligible increase rate and the amounts of CaO, BaSO₄, Ca₃Al₂O₆, CaAl₂O₄, Ca₁₂Al₁₄O₃₃, BaAl₂O₄, CaSO₄ are relatively large with a total content of over 50%. Gypsum cannot react completely at 1200 °C and 1300 °C. When the sintering temperature is 1350 °C and 1400 °C, the proportion of $Ca_{4-x}Ba_xAl_6SO_{16}$ is significantly increased; moreover, it increases with the

increase of prolonged time, and the mesophases are rapidly reduced. When the prolonged time is 180 min at 1400 °C, $\text{Ca}_{4-x}\text{Ba}_x\text{Al}_6\text{SO}_{16}$ accounts for approximately 88.4%. However, the amounts of $\text{Ca}_{4-x}\text{Ba}_x\text{Al}_6\text{SO}_{16}$ decreased at 1440 °C due to the decomposition. The content of gypsum is less than 1% when sintered for 180 min at 1350 °C and 1400 °C. CaSO_4 , free BaO and CaO formed at 1440 °C due to the decomposition of CBSA.

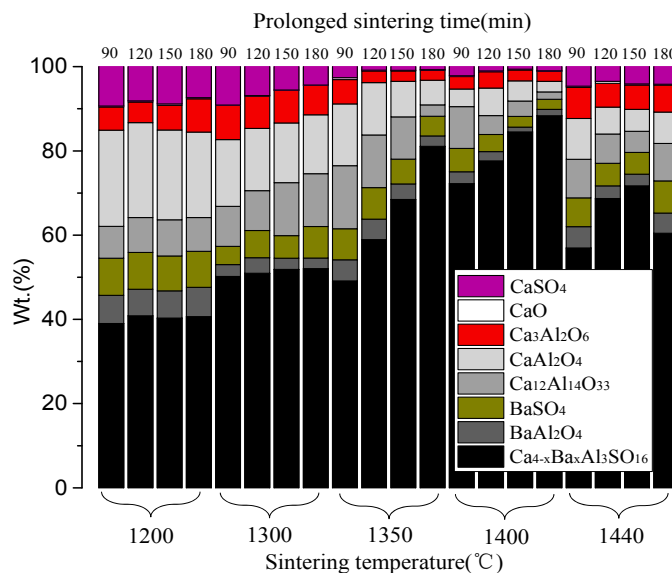


Figure 3. Results of quantitative analysis.

As is shown in Figure 4, the replacement rate of Ba^{2+} shows serious dependence on the sintering system. It maintained at less than 20% ignoring the increasing prolonged sintering time when sintered at 1200 °C and 1300 °C. At relatively low sintering temperature (1200 °C and 1300 °C), not all the Ba^{2+} can bound with CSA and the extra Ba^{2+} exists as other mesophases, such as BaAl_2O_4 , BaSO_4 . The replacement rate of Ba^{2+} increases with increasing sintering temperature and prolonged sintering time in the 1350–1400 °C range. In this sintering range, both the content of $\text{Ca}_{4-x}\text{Ba}_x\text{Al}_6\text{SO}_{16}$ and the replacement rate of Ba^{2+} increase rapidly. The replacement rate is about 80% when the sintered at 1400 °C for 180 min. The replacement rate also decreases due to the decomposition of $\text{Ca}_{4-x}\text{Ba}_x\text{Al}_6\text{SO}_{16}$.

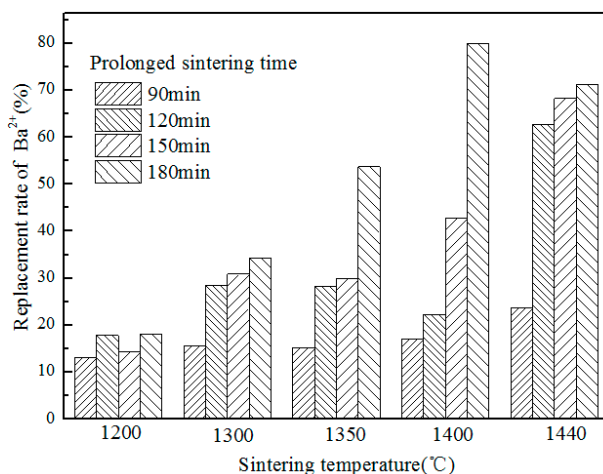


Figure 4. Replacement rate of Ba^{2+} at different sintering system.

From the correspondence between the content of $\text{Ca}_{4-x}\text{Ba}_x\text{Al}_6\text{SO}_{16}$ and replacement rate of Ba^{2+} , the two indexes arrived at the maximum under the same sintering system. Sintering at 1400 °C for 180 min is considered the optimum and $\text{Ca}_{3.2}\text{Ba}_{0.8}\text{Al}_6\text{SO}_{16}$ with a content of 88.4% was synthesized.

3.3. The Result of Strength

According to the water-cement ratio ($w/c = 0.5$), we mixed the clinker with the sintering temperature of 1350 °C and 1400 °C and put the paste into a $2 \times 2 \times 2$ cm mold by vibration. The specimens are unmolded after being cured in more than 90% moist air at 20 °C for 1 day. Then the specimens are cured in standard conditions for measurement of the compressive strength of 3 days and 7 days. The results are shown in Figure 5. We can see that the compressive strength increases with the increase of sintering temperature and the prolonged time.

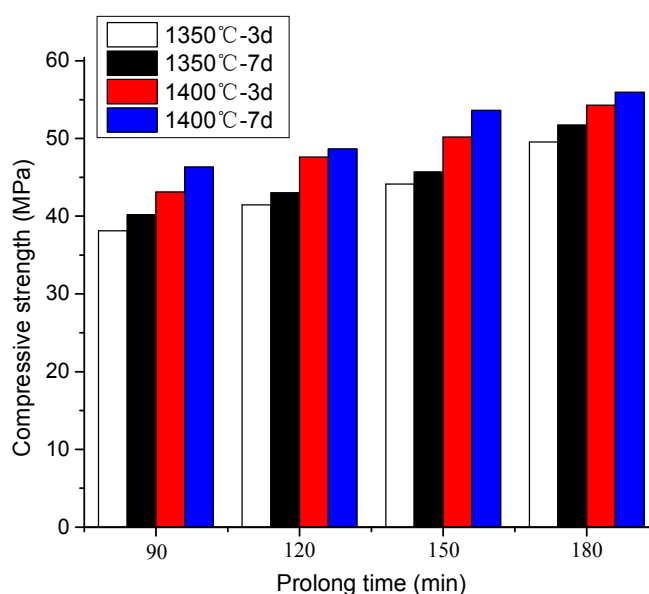


Figure 5. Compressive strength of 1350 °C and 1400 °C sintered clinkers.

4. Conclusions

(1) In the sintering process of calcium barium sulphoaluminate (CBSA) mineral, except for orthorhombic and cubic CBSA, there also exists mesophases including CaO , BaSO_4 , $\text{Ca}_3\text{Al}_2\text{O}_6$, CaAl_2O_4 , $\text{Ca}_{12}\text{Al}_{14}\text{O}_{33}$, BaAl_2O_4 , CaSO_4 . The content of CBSA shows serious dependence on the sintering system. When sintered at 1400 °C for 180 min, the content of CBSA reaches 88.4%. A higher sintering temperature will lead to the decomposition.

(2) Not all the Ba ions can be bounded with CSA in the sintering process. The replacement rate of Ba^{2+} increased with the increasing sintering temperature and prolonged sintering time and it reached the maximum when sintered at 1400 °C for 180 min.

(3) Considering the sintering content of CBSA and replacement rate of Ba^{2+} , the best sintering system is a prolonged sintering time of 180min at 1400 °C. The sintering content of CBSA is 88.4% and the replacement rate of Ba^{2+} is 80%. $\text{Ca}_{3.2}\text{Ba}_{0.8}\text{Al}_6\text{SO}_{16}$ was synthesized.

Acknowledgments

This work was financed by National Natural Science Foundation of China (51472041).

Author Contributions

Jun Chang put forward the main ideas of this paper and analyzed experimental results in theory. Xiaopeng Shang constituted and carried out the experiments; Shang also analyzed experimental results with software and wrote paper. All the authors read and approved the final manuscript.

Conflicts of Interest

The authors declare no conflict of interest.

Reference

1. Tereanu, I.; Munten, M.; Dragnea, I. Type $3(\text{CaO} \cdot \text{Al}_2\text{O}_3) \cdot \text{M}_x(\text{SO}_4)_y$ compounds and compatibility relations in $\text{CaO}-\text{CaO} \cdot \text{Al}_2\text{O}_3-\text{M}_x(\text{SO}_4)_y$ system. *Cement* **1986**, *83*, 39–45.
2. Yan, P. Hydration of Sr and Ba-bearing sulfoaluminates in the presence of sulphates. *Adv. Cem. Res.* **1993**, *5*, 65–69.
3. Chang, J. Study on new type Ba-bearing cement. Mater's Thesis, Wuhan University of Technology, Wuhan, China, 1998.
4. Cheng, X.; Chang, J.; Lu, L.; Liu, F.; Teng, B. Study of Ba-bearing calcium sulfoaluminate minerals and cement. *Cem. Concr. Res.* **2000**, *30*, 77–81.
5. Young, R.A. *The Rietveld Method*; Oxford University Press: Oxford, UK, 1993; pp. 21–22.
6. Halstead, P.E.; Moore, A.E. The composition and crystallography of an anhydrous calcium aluminosulphate occurring in expanding cement. *J. Appl. Chem.* **1962**, *12*, 413–417.
7. Saalfeld, H.; Depmeier, W. Silicon-free compounds with sodalite structure. *Krist. Tech.* **1972**, *7*, 229–233.
8. Calos, N.J.; Kennard, C.H.L.; Whittaker, A.K.; Davis, R.L. Structure of calcium aluminate sulfate $\text{Ca}_4\text{Al}_6\text{O}_{16}$ S. *J. Solid State Chem.* **1995**, *119*, 1–7.
9. Zhang, P.; Chen, Y.; Shi, P.; Wang, J. The crystal structure of $\text{C}_4\text{A}_3\text{S}$. In Proceedings of 9th International Congress on the Chemistry of Cement, New Delhi, India, 23–28 November 1992; 201–208.
10. Krstanović, I.; Radaković, A.; Karanović, L. X-Ray Powder Data for $\text{Ca}_4\text{Al}_6\text{O}_{12}\text{SO}_4$. *Powder Diffr.* **1992**, *7*, 47–48.
11. Hargis, C.W.; Moon, J.; Lothenbach, B.; Winnefeld, F.; Wenk, H.R.; Monterio, P.J. Calcium Sulfoaluminate Sodalite ($\text{Ca}_4\text{Al}_6\text{O}_{12}\text{SO}_4$) Crystal Structure Evaluation and Bulk Modulus Determination. *J. Am. Ceram. Soc.* **2014**, *97*, 892–898.
12. Cuesta, A.; de La Torre, A.G.; Losilla, E.R.; Peterson, V.K.; Rejmak, P.; Ayuela, A.; Aranda, M.A. Structure, atomistic simulations, and phase transition of stoichiometric yeelimite. *Chem. Mater.* **2013**, *9*, 1680–1687.
13. Cuesta, A.; de La Torre, A.G.; Losilla, E.R.; Santacruz, I.; Aranda, M.A. Pseudo cubic crystal structure and phase transition in doped yeelimite. *Cryst. Growth Des.* **2014**, *10*, 5158–5163.

14. Andac, O.; Glasser, F.P. Polymorphism of calcium sulphoaluminate ($\text{Ca}_4\text{Al}_6\text{O}_{16}\text{SO}_3$) and its solid solutions. *Adv. Cem. Res.* **1994**, *22*, 57–60.
15. Álvarez-Pinazo, G.; Cuesta, A.; García-Maté, M.; Santacruz, I.; Losilla, E.R.; de La Torre, A.G.; Aranda, M.A. Rietveld quantitative phase analysis of Yeelimite-containing cements. *Cem. Concr. Res.* **2012**, *7*, 960–971.
16. Jansen, E.; Schäfer, W.; Will, G. R values in analysis of powder diffraction data using Rietveld refinement. *J. Appl. Crystallogr.* **1994**, *4*, 492–496.
17. Ma, S.; Shen, X.; Huang, Y.; Huang, Y.; Zhong, B. Preparation and formation mechanism of calcium sulphoaluminate. *J. Ceram. Soc.* **2008**, *1*, 78–81.
18. Zhang, W.; Ouyang, S.; Chen, Y. Study on the compound formation in system $\text{CaO}-\text{Al}_2\text{O}_3-\text{BaSO}_4$ and the formation kinetics of $3\text{CaO}_3 \cdot \text{Al}_2\text{O}_3 \cdot \text{BaSO}_4$. *J. Chin. Ceram. Soc.* **2001**, *4*, 305–308.

© 2015 by the authors; licensee MDPI, Basel, Switzerland. This article is an open access article distributed under the terms and conditions of the Creative Commons Attribution license (<http://creativecommons.org/licenses/by/4.0/>).